

Liu Bing (Orcid ID: 0000-0002-3144-5673)

Title Page

Diosmetin induces apoptosis and enhances the chemotherapeutic efficacy of paclitaxel in non-small cell lung cancer cells via Nrf2 inhibition

Xiangcui Chen^{1,2,3#}, Qipeng Wu^{1,2,3#}, Yueming Chen^{1,2,3#}, Jiahao Zhang^{1,2,3}, Huachao Li^{1,2,3}, Zhicheng Yang^{1,2,3}, Yang Yang^{1,2,3}, Yanchao Deng^{1,2,3}, Luyong Zhang^{2,3,4*}, Bing Liu^{1,2,3*}

¹ Department of Clinical pharmacy, School of Pharmacy, Guangdong Pharmaceutical University, Guangzhou 510006, China

² Guangzhou key laboratory of construction and application of new drug screening model systems, Guangdong Pharmaceutical University, Guangzhou 510006, China

³ Key Laboratory of New Drug Discovery and Evaluation of ordinary universities of Guangdong province, Guangdong Pharmaceutical University, Guangzhou 510006, China

⁴ The Center for Drug Research and Development, Guangdong Pharmaceutical University, Guangzhou 510006, China

#Note: Xiangcui Chen, Qipeng Wu and Yueming Chen made equal contributions to this work.

*Corresponding authors: Bing Liu, Email: liubing520@gdpu.edu.cn; liubing52000@163.com. Tel: 86-20-39352128, Fax: 86-20-39352128. Luyong Zhang, Email: lyonzhong@163.com. Tel: 86-20-39352100, Fax: 86-20-39352100.

Running Title: Diosmetin induces apoptosis and enhances paclitaxel efficacy

This article has been accepted for publication and undergone full peer review but has not been through the copyediting, typesetting, pagination and proofreading process which may lead to differences between this version and the Version of Record. Please cite this article as doi: 10.1111/bph.14652

Abstract

Background and Purpose

Non-small cell lung cancer (NSCLC) accounts for up to 80–85% of all lung cancers with a disappointing prognosis. Flavonoids exert anti-cancer properties, mostly involving stimulation of ROS production without significant toxicity to normal cells. This study was aimed to delineate the effect of diosmetin, a natural flavonoid, on NSCLC cells and the ability to enhance the anti-tumour activity of paclitaxel.

Experimental Approach

NSCLC cells, normal cell lines HLF-1 and BEAS-2B, as well as immunodeficient mice were chosen as a model to study the treatment effects. Changes in cell viability, apoptosis and ROS were analyzed by MTT assay, flow cytometry assay and fluorescent probe DCFH-DA. Molecule expression was determined by western blotting and real-time RT-PCR. Xenografted tumors, spleens and other vital organs were harvested and subjected to growth inhibition measurement, histological and immunohistochemical analyses.

Key Results

Diosmetin induced selective apoptotic death in NSCLC cells, but spared normal cells, via ROS accumulation. Diosmetin induced ROS production in NSCLC cells probably via reducing Nrf2 stability through disruption of PI3K/Akt/GSK-3 β pathway. The *in vitro* and *in vivo* xenograft studies showed that combined treatment of diosmetin and paclitaxel synergistically suppressed NSCLC cells. Histological analysis of vital organs showed no obvious toxicity of diosmetin,

which matched our *in vitro* findings.

Conclusions and Implications

Diosmetin selectively induces apoptosis and enhances the paclitaxel efficacy in NSCLC cells via ROS accumulation through disruption of PI3K/Akt/GSK-3 β /Nrf2 pathway. Therefore, diosmetin may be a promising candidate for NSCLC adjuvant treatment.

Bullet point summary

What is already known

Flavonoids exert anti-cancer properties, mostly involving stimulation of ROS production without toxicity to normal cells.

What this study adds

Diosmetin induces apoptosis and enhances paclitaxel efficacy in NSCLC via ROS accumulation through PI3K/Akt/GSK-3 β /Nrf2 pathway.

Clinical significance

Diosmetin may be a promising anticancer candidate for NSCLC adjuvant treatment.

Abbreviations

NSCLC, non-small cell lung cancer; ROS, reactive oxygen species; IC₅₀, half-maximal inhibitory concentration; DCFH-DA, 2',7'-dichlorodihydrofluorescein diacetate; NAC, N-acetylcysteine; Nrf2, NF-E2-related factor 2; HO1, heme oxygenase; NQO1, NAD(P)H dehydrogenase, quinone 1; tBHQ, Tert-butyl-hydroquinone; GSK-3 β , glycogen synthase kinase-3 β

Introduction

Lung cancer ranks first in cancer-related mortalities worldwide. Non-small cell lung cancer (NSCLC) accounts for up to 80–85% of all lung cancer cases with a disappointing prognosis (Chen *et al.*, 2014). Although recent advances in chemotherapy with a platinum agent in combination with other cytotoxic agents and targeted therapies have yielded modest improvements in NSCLC patient outcomes, the 5-year overall survival rate remains frustratingly poor due to the associated dose limiting toxicities and acquisition of drug resistance (Latimer *et al.*, 2015). Therefore, there is an urgent need to develop new effective adjuvant therapy with minimal adverse effects against NSCLC.

Cancer cells are characterized by high levels of reactive oxygen species (ROS) compared with their normal counterparts (Moloney *et al.*, 2017). A moderate increase in ROS promotes cell proliferation, whereas excessive amounts of ROS cause toxicity to cancer cells (Raza *et al.*, 2017). Cancer cells with increased oxidative stress are likely to be more vulnerable to damage by further ROS insults. Therefore, manipulation of ROS levels is a promising strategy to selectively kill cancer cells without significant toxicity to normal cells (Schumacker *et al.*, 2006).

Therapeutic intervention by developing new phytochemicals which are effective, nontoxic and cost-effective is an emerging field in cancer management (Deep *et al.*, 2008). Flavonoids account for the largest and most ubiquitous group of secondary plant metabolites and are widely distributed in plants. Extensive and increasing preclinical evidence has accumulated for their anticancer effect (Jiang *et al.*, 2018; Pan *et al.*, 2012; Park *et al.*, 2012). The anticancer effect of flavonoids has been reported to be through multiple mechanisms, however, stimulation of

ROS production constitutes the a widely accepted mechanism for their anticancer property (Kim *et al.*, 2016; Martinez-Perez *et al.*, 2016; Wang *et al.*, 2018). Diosmetin (5, 7-Trihydroxy-4'-methoxyflavone), a natural flavonoid present in legumes, olive leaves and other citrus plants, has anti-mutagenic and anti-allergic properties. Recently, several reports have shown the attractive cytotoxic activity of diosmetin on human cancer cells. For example, Oak et al. found that diosmetin displays anticancer activity in prostate cancer cells via inducing apoptosis and cell cycle arrest (Oak *et al.*, 2018). Besides, it was reported that diosmetin induces apoptosis in HepG2 cells by regulating CYP1A1/CYP1A2 due to p53 activation (Liu *et al.*, 2017). Nevertheless, the exact role of diosmetin in NSCLC cells and whether it has selective toxic effect on cancer cells remains unclear.

This study was designed to explore the potential toxicity of diosmetin in NSCLC cells and the underlying mechanism. Our data demonstrate that diosmetin effectively induces ROS-dependent NSCLC cell apoptosis via disruption of PI3K/Akt/GSK-3 β /Nrf2 pathway while it spares normal cells. Specifically, diosmetin enhances paclitaxel efficacy both *in vitro* and *in vivo*. Therefore, diosmetin may be a promising candidate for NSCLC adjuvant treatment.

Methods

Materials

Diosmetin (#S2380), MG132 (#S2619) and paclitaxel (#S1150, CAS Number: 33069-62-4) were purchased from Selleckchem. N-acetyl-L-cysteine (NAC) (#A7250, CAS Number: 616-91-1) and LiCl (#746460, CAS Number: 7447-41-8) were obtained from Sigma Chemical Co. Tert-Butylhydroquinone (tBHQ) (#150840025, CAS Number: 88-58-4)

and LY294002 (PI3K inhibitor) (#440206, CAS Number: 942289-87-4) were from Acros Organics and Merck, respectively. All other reagents were from Sigma Chemical Co. unless stated otherwise.

Cell lines and culture

Human NSCLC cell lines (A549 (RRID:CVCL_0023), H1299 (RRID:CVCL_0060), H460 (RRID:CVCL_0459), SPC-A1 (RRID:CVCL_6955), H441 (RRID:CVCL_1561), H1650 (RRID:CVCL_1483), Calu-3 (RRID:CVCL_0609)) and normal lung epithelial cells (BEAS-2B) (RRID:CVCL_0168) and human lung fibroblasts (HLF-1 (RRID:CVCL_KF72)) were originally from ATCC. All NSCLC cell lines were cultured in Dulbecco's modified Eagle's medium (DMEM, Gibco-BRL, Gaithersburg, MD, USA). BEAS-2B cells were cultured in epithelia cell medium (Gibco-BRL, Gaithersburg, MD, USA). HLF-1 cells were cultured in Roswell Park Memorial Institute-1640 medium (RPMI-1640, Gibco-BRL, Gaithersburg, MD, USA). All of them were supplemented with 10% fetal bovine serum (FBS) and penicillin/streptomycin. Cells were cultured in a standard humidified incubator at 37°C in a 5% CO₂ atmosphere.

Cell viability, IC₅₀ calculation and reactive oxygen species (ROS) assay

The protocol used for MTT assay of detection of cell viability was strictly according to our previous study (Zhang *et al.*, 2014). Briefly, 5×10^4 cells in 100 µL of serum-free culture medium were seeded in 96-well plates and incubated for 48 hours with individual treatment. Then, MTT was added to each well (with a final concentration of 0.5 mg/ml). After incubation at 37°C for 4 hours, the plates were centrifuged at $450 \times g$ for 5 mins. Untransformed MTT was removed by aspiration, and formazan crystals were dissolved in dimethyl sulfoxide (150

µl/well), quantified spectrophotometrically at 563 nm.

For assays determining IC₅₀ for diosmetin, the cell viability was measured by MTT in the presence of a wide range of concentrations of diosmetin (5 µM – 55 µM). All assays were performed in triplicate and data is reported as mean and standard deviation. Product formation data (% activity, 100% = activity in absence of diosmetin) and plotted versus log of diosmetin concentration. The resulting data values were fit by non-linear regression to the equation ($y = a/(1 + \exp(-(x-x_0)/b))$) for a sigmoidal curve, and the diosmetin concentrations corresponding to 50% activity were determined from the regression parameters.

The intracellular ROS was measured using a fluorescent probe DCFH-DA. After multiple treatments for 12 hours, A549, H1299 and BEAS-2B cells were washed with cold PBS and suspended in PBS at 5×10^5 cells/mL. Then, the cells were incubated with DCFH-DA (5 µM) for 40 mins at 37 °C in the darkness. The fluorescence intensity of each well was quantified with a fluorescence microplate reader (HITACHI, 650-60, Tokyo, Japan) at $E_x/E_m = 485/530$ nm.

Flow cytometry (FCM) analysis of apoptosis

Apoptotic cell death was determined by flow cytometry analysis using Annexin V-FITC and propidium iodide (PI) assay kit (BD, PharMingen, San Diego, CA). After 24-hour individual drug treatment, A549, H1299 and BEAS-2B cells were collected, washed with cold PBS, suspended in 5 µL of Annexin V binding buffer and stained with 5 µL of PI. The cells were mixed gently, incubated in the dark for 20 mins, and washed. The samples were analyzed with a FACS (Beckman Coulter, CA).

ARE-luciferase reporter assay

The ARE-luciferase reporter assay protocol was according to our previous study (Wu *et al.*, 2017). Briefly, A549, H1299 and BEAS-2B cells were transduced with the Cignal ARE reporter (SABiosciences, Frederick, MD). Luciferase activity was measured by dual-luciferase reporter gene assay system (Promega) according to the manufacturer's protocol. Results were presented as firefly luciferase activity.

Nrf2 plasmid transfection

For transfection of Nrf2 overexpressing plasmid, the pCDNA3-Myc3-Nrf2 plasmid (Addgene; Plasmid number: 21555) was transfected into A549 and H1299 cells together with Lipofectamine 2000 (Invitrogen, 11668-019) overnight according to manufacturer's instructions, and then cultured for 10 days with 500 µg/ml G418 after infection. The positive clones were collected for further study.

Western blotting

After individual drug treatment for indicated period, the whole cell extracts were obtained by using cell lysis buffer (Cell Signaling Technology, Beverly, MA, USA) with 0.5% protease inhibitor cocktail (Sigma, St Louis, MO, USA) and 1% phosphatase inhibitor cocktail I (Sigma). The membranes were first probed with primary antibodies as follows: anti-Nrf2 antibody (Abcam Cat#ab31163, RRID:AB_881705), anti-p-Akt antibody (Cell signaling Cat#4060, RRID:AB_2315049), anti-p-GSK3 β (Ser9) antibody (Cell signaling Cat#9323, RRID:AB_2115201), anti-Bax antibody (Cell signaling Cat# 14796, RRID:AB_2716251), anti-Bcl-2 antibody (Cell signaling Cat#3498, RRID:AB_1903907), anti-Akt antibody (Cell signaling Cat#4685, RRID:AB_2225340), anti-GSK3 β antibody (Cell signaling Cat#5676,

RRID:AB_10547140) and anti- β -tubulin antibody (Abcam Cat# ab6046, RRID:AB_2210370). For analysis of Nrf2, p-Akt and p-GSK-3 β (Ser9), blots were probed with their specific antibodies (diluted with 5% BSA to 1: 1000). For analysis of β -tubulin, blots were probed with its antibody (diluted with 5% BSA to 1: 5000). Membranes were probed with horseradish peroxidase (HRP)-labeled anti-rabbit secondary antibody from Cell Signaling (diluted with 5% BSA to 1: 1000). Antibody binding was detected by enhanced chemiluminescence detection kit (ECL) (UK Amersham International plc).

Real-time RT-PCR

Total RNA was extracted from A549, H1299 and BEAS-2B cells using Trizol Reagent (Invitrogen), and then complementary DNA (cDNA) was synthesized using ReverTra Ace reverse transcriptase (TOYOBO, Japan, FSQ-301) according to the manufacturer's protocol. Real-time RT-PCR was performed with the SYBR Green Realtime PCR Master Mix (TOYOBO, Japan, QPK-201) on an iCycler (Bio-Rad) following the manufacturer's instructions. The primer sequences were as follows: Nrf2 forward primer: GACGTGTGGCGGCTGAGC; Nrf2 reverse primer: GCACCG CGTCCGA ACTAGAAG; GAPDH forward primer: GGCACCGTCAAGGCTGAGA AC; GAPDH reverse primer: CATGGTGGTGAAGACGCCAGTG; HO-1 forward primer: GGTGCTCGTACTGCTACTGTTCATG; HO-1 reverse primer: GCCACGAA CCTCATCTCTTCCAC; NQO-1 forward primer: CGCCTGCCATCATGCCTGAC; NQO-1 reverse primer: GTGTGGTGGATCACGCCTGTAATC. The gene expression levels for each amplification were calculated using the $\Delta\Delta$ CT method and normalized against GAPDH mRNA.

Determination of combination index and dose reduction index

The interaction between diosmetin and paclitaxel was determined by the combination index (CI), which was calculated according to the median-effect principle according to a previous report (Chou *et al.*, 1984). The equation for the isobologram was shown as $CI = (D)_1/(Dx)_1 + (D)_2/(Dx)_2$. $(Dx)_1$ and $(Dx)_2$ indicated the individual doses of diosmetin and paclitaxel required to inhibit a given level of cell viability, and $(D)_1$ and $(D)_2$ were the doses of diosmetin and paclitaxel necessary to produce the same effect in combination, respectively. The combination effects of diosmetin and paclitaxel were indicated as follows: $CI < 1$, synergism; $CI = 1$, additive effect; and $CI > 1$, antagonism. The dose reduction index (DRI) was defined by the level of dose reduction in a combination for a given level of effect as compared to the concentration of individual drug alone. The equation for the DRI was shown as follows: $(DRI)_1 = (Dx)_1 / (D)_1$ and $(DRI)_2 = (Dx)_2 / (D)_2$.

In vivo anti-tumor efficacy assay

The animal experiment was approved by the Animal handling and procedures were approved by the Guangdong Animal Center (No. GDP20170224). All animal experiments complied with the National Institutes of Health guide for the care and use of Laboratory animals (NIH Publications No. 8023, revised 1978). A549 cells (approximately 2×10^6 cells) were subcutaneously inoculated into the right flank of 6-week-old female nude mice. When the tumors had developed to about 80-100mm³, the mice were divided into five groups (n=5 per group). The mice were differently treated with diosmetin (50 mg/kg, thrice weekly, by intraperitoneal injection), diosmetin plus NAC (7 mg/ml given in the drinking water for the length of the experiment), paclitaxel (10 mg/kg, thrice weekly, by intraperitoneal injection), or

diosmetin plus paclitaxel, respectively. The therapy was continued for 4 weeks. The body weight and tumor size were measured and calculated once every two days. The mice were sacrificed 4 weeks after the initiation of treatment. Tumor and organ tissues (liver, heart, lung, spleen and kidney) were collected for H&E staining and immunostaining analyses of Nrf2 and Ki67 (anti-Ki67 antibody, Abcam Cat# ab15580) expression. Tumor tissue ROS were measured using the probe H2DCFDA as described in a previously published report.

TUNEL staining

The TUNEL staining was performed with the In situ cell death detection kit (Roche, Basel, Switzerland) according to the manufacturer's instructions. After 15-min incubation with Proteinase K (20 mg/ml) at room temperature, the sections were incubated with 2% H₂O₂ for 5 min to block endogenous peroxidase. Then sections were incubated with the TdT enzyme at 37 °C for 2 h. After 30-min incubation with antidigoxin–peroxidase solution, the sections were stained with diaminobenzidine (DAB) substrate for 2 min and then counterstained with hematoxylin. Thereafter, slides were photographed with a microscope camera system.

Statistical analysis

Experimental data were presented as mean ± S.D. from five independent experiments and were analyzed with the unpaired Student's t test by using GraphPad 5 Software (RRID:SCR_002798). *P* value of <0.05 was considered statistically significant. For the *in vivo* study, a log-linear mixed model with random intercept was used to compare the significance of the mean tumor volumes among each group.

Results

Diosmetin selectively reduces NSCLC cell viability and induces cell apoptosis via cellular

ROS accumulation

The structure of diosmetin with the molecular weight of 300.26 g/mol used in this study was shown in Fig. 1A. Fig. 1B shows that diosmetin treatment for 48 hours markedly reduced the viability a panel of 7 different NSCLC cell lines in a dose-dependent manner determined by MTT assay, with the indicated half-maximal inhibitory concentration (IC_{50}) ranging from $11.01 \pm 0.28 \mu\text{M}$ to $33.60 \pm 0.84 \mu\text{M}$. However, diosmetin had little cytotoxicity in 2 normal cell lines (HLF-1 and BEAS-2B) with the same concentration ranges used in NSCLC cell lines. Fig. 1C shows that diosmetin ($20 \mu\text{M}$) reduced the viability of A549 and H1299 cells via a time-dependent manner (ranged from 24 to 72 hours).

To explore whether diosmetin exerts its cytotoxic effects in NSCLC cells via ROS elevation, we first sought to determine the effect of diosmetin on ROS production in NSCLC cells. Fig. 2A shows that diosmetin dose-dependently enhanced ROS production in A549 and H1299 cells, while had no or little effect on ROS production in BEAS-2B cells (Fig. 2B). The enhancement of diosmetin on ROS accumulation in A549 and H1299 cells was efficiently abrogated by administration of a ROS scavenger NAC (25 mM) (Fig. 2C). To clarify the mechanism for suppression of NSCLC cell viability by diosmetin, we next determined whether it could induce apoptosis in A549 and H1299 cells. As shown in Fig. 2D and Fig. 2F, after 24-hour treatment, diosmetin induced apoptosis in A549 and H1299 cells in a dose-dependent manner determined by flow cytometry assay. Besides, diosmetin significantly promoted the pro-apoptotic protein Bax expression while reduced the anti-apoptotic protein Bcl-2 expression via a concentration-

dependent manner after 24-hour treatment in A549 and H1299 cells (Fig. 2E and Fig. 2G). On the contrary, diosmetin elicited little or no pro-apoptotic effect on BEAS-2B cells at the same doses used in NSCLC cells (Fig. 2H). Additional administration of NAC (25 mM) could efficiently reverse the effect of diosmetin (20 μ M) on A549 and H1299 cell apoptosis (Fig. 2D and Fig. 2E). Furthermore, the inhibition of diosmetin on A549 and H1299 cell viability was also blocked by NAC treatment determined by MTT assay (Fig. 2G).

Therefore, these results strongly support that diosmetin selectively kills NSCLC cells but spares normal cells through ROS-mediated apoptosis.

Interference of Nrf2 expression mediates diosmetin-induced NSCLC cell apoptosis

To further determine the mechanism for diosmetin-induced ROS accumulation and resultant NSCLC cell apoptosis, we then sought to examine the effect of diosmetin on Nrf2 expression as many flavonoids cause ROS burst in cancer cells via inhibition of Nrf2 (Kittiratphatthana *et al.*, 2017; Mostafavi-Pour *et al.*, 2017; Wang *et al.*, 2017). Fig. 3A and Fig. 3B show that diosmetin treatment for 12 hours could efficiently suppress Nrf2 expression at the protein level in a dose-dependent manner but had no effect on Nrf2 mRNA expression in A549 and H1299 cells. By means of ARE reporter gene assay and real-time RT-PCR, we found that diosmetin dose-dependently reduced ARE-luciferase activity (Fig. 3C) and repressed the mRNA levels of Nrf2-targeted genes including heme oxygenase (HO1) and NAD(P)H dehydrogenase, quinone 1 (NQO1) (Fig. 3D). Nevertheless, diosmetin slightly enhanced Nrf2 expression (Fig. 3E) and ARE-luciferase activity (Fig. 3F) in BEAS-2B cells.

Tert-butyl-hydroquinone (tBHQ) is a well-recognized Nrf2 activator (Ye *et al.*, 2016). Fig. 4A shows that tBHQ administration for 12 hours resulted in a dose-dependent increase in Nrf2

activity in A549 and H1299 cells determined by ARE-luciferase reporter assay. Next, we sought to detect whether tBHQ could counteract diosmetin effects in NSCLC cells. As shown in Fig. 4B, additional tBHQ treatment (20 μ M) efficiently reversed diosmetin-induced ROS accumulation in A549 and H1299 cells. Furthermore, tBHQ could significantly rescue diosmetin (20 μ M)-induced apoptosis in these cells (Fig. 4C). To further confirm our finding, we transfected A549 and H1299 cells with Nrf2 overexpressing plasmid. Fig. 4D displays the transfection efficiency of Nrf2 plasmid. Similar with tBHQ, Nrf2 overexpression significantly reversed diosmetin-induced ROS accumulation (Fig. 4E) and apoptosis (Fig. 4F) in A549 and H1299 cells.

Therefore, these data suggest that diosmetin induces NSCLC cell apoptosis via suppression of Nrf2 expression and resultant ROS accumulation.

Diosmetin attenuates Nrf2 expression in NSCLC cells via PI3K/Akt/GSK-3 β pathway

The finding that diosmetin reduced Nrf2 expression at the protein level but not at the mRNA level strongly suggests that diosmetin may interfere Nrf2 stability. To further confirm this assumption, we sought to determine the effect of the proteasome inhibitor MG132 on diosmetin-decreased Nrf2 expression. As shown in Fig. 5A, MG132 (10 μ M) treatment alone enhanced Nrf2 expression, and rescued the reducing effect of diosmetin on Nrf2 expression in A549 and H1299 cells. Nrf2 degradation and instability are regulated by Keap1 and glycogen synthase kinase-3 β (GSK-3 β) (Hayes *et al.*, 2015). In the present study, both A549 and H1299 cells harbor Keap1 mutation that disturbs inhibitory Nrf2-Keap1 interaction for subsequent proteasome-dependent degradation of Nrf2. GSK-3 β is negatively regulated by PI3K/Akt axis via phosphorylation at Serine 9 (Ser 9) (Wang *et al.*, 2016). Therefore, we determined whether

diosmetin interferes Nrf2 stability via PI3K/Akt/GSK-3 β pathway.

Fig. 5B shows that diosmetin dose-dependently reduced Akt phosphorylation and GSK-3 β phosphorylation at Ser 9 after 8-hour incubation. Treatment with LY294002 (30 μ M), a selective inhibitor of PI3K/Akt pathway, exerted a similar inhibitory effect on Nrf2 expression compared with diosmetin after 12-hour administration (Fig. 5C). When PI3K/Akt pathway activity was suppressed by LY294002, diosmetin (20 μ M) treatment could not further decrease the Nrf2 protein level. The similar trends were also found in ARE-luciferase activity (Fig. 5D), as well as HO-1 and NQO-1 mRNA expression (Fig. 5E). Fig. 5F-5H show that additional treatment with LiCl (30 mM), a potent inhibitor of GSK-3 β (Gao *et al.*, 2017), efficiently blocked the inhibitory effect of diosmetin on Nrf2 expression, ARE-luciferase activity, as well as HO-1 and NQO-1 mRNA expression, respectively. Taken together, the above data suggest that diosmetin regulates Nrf2 in a PI3K/Akt/GSK-3 β -dependent manner.

Diosmetin enhances paclitaxel cytotoxicity in NSCLC cells

As accumulation of ROS is the crucial step for paclitaxel-induced cancer cell death (Alexandre *et al.*, 2006), we next sought to determine whether diosmetin could sensitize NSCLC cells to paclitaxel. The viability of A549 and H1299 cells treated with diosmetin and paclitaxel was assessed after 48-hour treatment.

As seen in Fig. 6A, paclitaxel reduced the viability of A549 and H1299 cells in a dose-dependent manner with the IC₅₀ of 271.81 nM and 249.63 nM, respectively. To evaluate the potential synergistic effect of diosmetin and paclitaxel, we subjected A549 and H1299 cells to diosmetin with the concentration equal to its half IC₅₀ (5 μ M) in combination with a lower dose (120 nM) of paclitaxel in the subsequent studies. Fig. 6B shows that a greater antiproliferative

effect of diosmetin was observed in paclitaxel-treated A549 and H1299 cells compared with treatments using diosmetin or paclitaxel alone. Besides, as expected, combination treatment resulted in a significant increase in ROS content compared with each treatment alone (Fig. 6C).

The fraction-effect versus combination index (FA–CI) curve shown in Fig. 6D demonstrated the synergistic ($CI < 1$) cytotoxic effect of diosmetin combined with paclitaxel, with CI values in A549 cell ranging from 0.401992 to 1.07626 and in H1299 cell ranging from 0.59862 to 1.07068 at different drug combination doses from 0.25*ED50 to 4*ED50. Combining diosmetin and paclitaxel resulted in a favorable DRI, ranging from a 1.1- to 6.9-fold dose reduction for both drugs (supplementary table 1). Therefore, analysis of the enhanced efficacy obtained by combining diosmetin and paclitaxel indicated synergism.

Diosmetin impairs A549 cells and enhances paclitaxel efficacy *in vivo*

To extend our *in vitro* observations, we investigated whether diosmetin impairs NSCLC cells and augments paclitaxel toxicity *in vivo*. A549 cells (approximately 2×10^6 cells) were subcutaneously inoculated into the right flank of 6-week-old female nude mice. When tumors grew to 80-100 mm³, the mice were differently treated with diosmetin (50 mg/kg, thrice weekly, by intraperitoneal injection), diosmetin plus NAC (7 mg/ml given in the drinking water for the length of the experiment), paclitaxel (10 mg/kg, thrice weekly, by intraperitoneal injection), or diosmetin plus paclitaxel, respectively.

After 28-day treatment, we observed inhibition of tumor growth with diosmetin and paclitaxel alone (Fig. 7A-7C). The administration of ROS scavenger NAC significantly rescued diosmetin-elicited tumor inhibition. The combination of diosmetin and paclitaxel enhanced this inhibitory effect on tumor growth compared with single treatments. Histological

analysis of heart, liver, spleen, lung and kidney tissues (Fig. 7D) showed no alterations between control group and diosmetin treatment group, suggesting that diosmetin did not produce any toxic effects in normal tissues, which matched our *in vitro* findings. Furthermore, the results proved that Nrf2 and Ki67 levels were reduced, while the TUNEL staining was upregulated in diosmetin-treated xenograft tumor tissues determined by IHC (Fig. 7E). To determine whether the same anti-tumor mechanisms exist in the xenograft model as our *in vitro* studies, we assessed oxidative stress in tumor tissues, and found that either diosmetin or paclitaxel alone produced ROS accumulation compared with control group, additional NAC administration could reverse diosmetin effect on ROS production, and diosmetin plus paclitaxel treatment resulted in significant increase in ROS accumulation compared with single treatments (Fig. 7F).

Discussion

Many anticancer drugs fail in selectivity for cancer cells as damage both cancer and normal cells, which results in many severe side effects. ROS levels are higher in cancer cells compared with those in normal cells. Normal cells can tolerate a certain level of ROS, however, cancer cells are likely to be more sensitive to damage by ROS-modulating drugs that increase ROS levels above the threshold of redox homeostasis (Gupte *et al.*, 2009). Many natural products have been found to achieve ROS-based selective cell killing for anticancer therapy (Chiu *et al.*, 2013; Kim *et al.*, 2016; Tang *et al.*, 2018). In the present study, we found that diosmetin selectively suppressed viability and induced apoptosis in NSCLC cells but spared normal cells; diosmetin enhanced ROS production in NSCLC cells, while had no or little effect on ROS production in normal cells; elimination of ROS efficiently rescued the pro-apoptotic effect on

NSCLC cells. These results strongly support that diosmetin treatment selectively induces apoptosis in NSCLC cells without general toxicity in normal cells via perturbing redox and ROS homeostasis in cancer cells.

Nrf2 is a transcription factor, belonging to the cap'n'collar (CNC) family and/or CNC-bZIP proteins. Nrf2 controls cellular antioxidant responses through its ability to regulate the expression of GSH metabolism-related enzymes (xCT, GCLC/GCLM, TXN, GS), the expression of enzymatic antioxidant systems (GPX, GR, PRX, and TRXR) and their cofactors (NADPH, FADH₂) to maintain redox homeostasis (Lee *et al.*, 2017). Many cancer cells thrive despite having high ROS levels by constitutively activating Nrf2, suggesting that targeting this transcription factor could be a good and promising therapeutic approach against cancer (Jung *et al.*, 2018). Specific to flavonoids, many agents like luteolin (Kittiratphatthana *et al.*, 2016), chrysin (Wang *et al.*, 2017) and quercetin (Mostafavi-Pour *et al.*, 2017) induce cancer cell apoptosis via inhibition of Nrf2. Our study found that diosmetin efficiently suppressed Nrf2 expression, ARE-luciferase activity as well as Nrf2-targeted genes expression in NSCLC cells. Activation of Nrf2 reversed diosmetin-induced ROS accumulation and apoptosis in these cells. These data imply that diosmetin induces NSCLC cell apoptosis via suppression of Nrf2 expression and resultant ROS accumulation. The antioxidant systems in cancer cells are very complex, including activation of redox-sensitive transcription factors, such as NF- κ B, Nrf2, c-jun and HIF-1, leading to the increased expression of various antioxidant molecules (Trachootham *et al.*, 2009). Therefore, we cannot necessarily exclude the possible involvement of other redox-sensitive transcription factors and antioxidant molecules in diosmetin-induced apoptosis in NSCLC cells. The comprehensive knowledge of the interference of diosmetin in

redox imbalance in cancer cells needed further clarified in future work.

This study found that diosmetin reduced Nrf2 expression at the protein level but not at the mRNA level, strongly suggesting that diosmetin may interfere Nrf2 stability. Nrf2 is bound to Kelch-like ECH-associated protein 1 (Keap1), which targets Nrf2 for its proteasomal degradation (Kobayashi *et al.*, 2005). However, in A549 and H1299 cells, Keap1 is mutated and its function in regulation of Nrf2 degradation is diminished. In addition to Keap1, Nrf2 is also repressed by β -transducin repeat-containing protein (β -TrCP), present in the Skp1–cullin-1–F-box protein (SCF) ubiquitin ligase complex SCF/ β -TrCP; SCF/ β -TrCP itself is enhanced by prior phosphorylation of the transcription factor by GSK-3 (Rada *et al.*, 2011). GSK-3 β is negatively regulated by PI3K/Akt axis via phosphorylation at Serine 9 (Ser 9) (Li *et al.*, 204; Wang *et al.*, 2016). As diosmetin has been confirmed to inhibit Akt activation in cancer cells including lung cancer cells (Xu *et al.*, 2017; Rebeca *et at.*, 2016), we assumed that whether diosmetin interferes Nrf2 expression via PI3K/Akt/GSK-3 β pathway. Our results indicated that diosmetin reduced Akt phosphorylation and GSK-3 β phosphorylation at Ser 9 in A549 and H1299 cells. Inhibition of PI3K/Akt pathway exerted a similar inhibitory effect on Nrf2 expression compared with diosmetin, and inhibitor of GSK-3 β efficiently blocked the inhibitory effect of diosmetin on Nrf2 expression. These data strongly suggest that diosmetin regulates Nrf2 in a PI3K/Akt/ GSK-3 β -dependent manner.

Diosmetin was reported to alleviate lipopolysaccharide-induced acute lung injury through stimulating the expression of Nrf2 and its target gene HO-1 (Liu *et al*, 2018) . Besides, diosmetin also exerts cytoprotective effects against hydrogen peroxide-induced L02 cell oxidative damage via activation of Nrf2 (Wang *et al.*, 2018). In addition to diosmetin, many

flavonoids exhibit the different effects on Nrf2 in cancer cells versus normal cells. For example, luteolin elicits a dramatic reduction in Nrf2 expression in human lung carcinoma A549 cells (Tang *et al.*, 2011) while induces protective effects against mercuric chloride-induced lung injury in mice via AKT-dependent Nrf2 activation (Liu *et al.*, 2018). Though we cannot definitely explain how the discrepancy arises, one possible explanation may be that many oncogenic pathways that flavonoids may influence in cancer cells are constitutively activated while remain the base-line level in normal cells. However, much work should be performed to clarify this issue in future studies.

It is superior to combine drugs inducing ROS generation with those abrogating the redox adaptation in cancer cells as to maximally benefit from the ROS-targeted therapeutic strategy (Trachootham *et al.*, 2009). Accumulation of ROS mainly via stimulation of the NADPH oxidase is a crucial involvement in paclitaxel cytotoxicity in cancer cells (Alexandre *et al.*, 2006; Alexandre *et al.*, 2007). Nrf2 is a well-known mediator of redox adaptation in cancer cells (Ciamporcero *et al.*, 2018; Rojo de la Vega *et al.*, 2018), and inhibition of Nrf2 enhances the paclitaxel chemosensitivity in cancer cells (Woo *et al.*, 2017). In this study, we found that combining diosmetin and paclitaxel resulted in synergistic effects on ROS accumulation and viability inhibition in NSCLC cells. Therefore, inhibition of Nrf2 by diosmetin may be a promising strategy to enhance paclitaxel sensitivity in NSCLC.

The present study clearly showed that diosmetin was as effective as paclitaxel at reducing A549 tumor *in vivo*, but the combination treatment was apparently more effective than either single-drug treatment. In addition, Nrf2 levels were reduced and ROS was elevated in diosmetin-treated xenograft tumor tissues. It also implied that diosmetin caused little toxicity

in organs. Therefore, because paclitaxel is currently a first-line agent for NSCLC chemotherapy, the use of diosmetin in combination with paclitaxel may be effective in a clinical setting to enhance chemosensitivity of paclitaxel and potentially reduce toxicity.

In conclusion, this study demonstrates that diosmetin selectively induces ROS accumulation and cell death, as well as enhances the antitumor efficacy of paclitaxel in NSCLC cells by interfering with Nrf2 antioxidant defense mechanisms through disruption of PI3K/Akt/GSK-3 β pathway. Therefore, diosmetin may be a promising anticancer candidate for NSCLC adjuvant treatment.

Acknowledgements

This work was supported by the project of the new star of Zhujiang science and technology (No. 201710010001), the National Natural Science Foundation of China (No. 81672836 and No. 81472205), the Open Project funded by Key laboratory of Carcinogenesis and Translational Research, Ministry of Education/Beijing (No. 2017 Open Project-2) and the Guangdong Key Laboratory of Pharmaceutical Bioactive Substances.

Author contributions

X.C., Q.W., Y.C., J.Z., H.L., Z.Y., Y.Y. and Y.D. carried out experiments. X.C., Q.W. and Y.C. analysed data. L.Z. and B.L. conceived experiments and wrote the paper. All authors had final approval of the submitted and published versions.

Conflict of interest

None.

Declaration of transparency and scientific rigour

This Declaration acknowledges that this paper adheres to the principles for transparent reporting and scientific rigour of preclinical research as stated in the BJP guidelines for Design & Analysis, Immunoblotting and Immunochemistry, and Animal Experimentation, and as recommended by funding agencies, publishers and other organisations engaged with supporting research.

Accepted Article

References

- Alexandre J, Batteux F, Nicco C, Chereau C, Laurent A, Guillevin L *et al.* (2006). Accumulation of hydrogen peroxide is an early and crucial step for paclitaxel-induced cancer cell death both *in vitro* and *in vivo*. *Int J Cancer* **119**(1): 41-48.
- Alexandre J, Hu Y, Lu W, Pelicano H, Huang P (2007). Novel action of paclitaxel against cancer cells: bystander effect mediated by reactive oxygen species. *Cancer Res* **67**(8): 3512-3517.
- Chen Z, Fillmore CM, Hammerman PS, Kim CF, Wong KK (2014). Non-small-cell lung cancers: a heterogeneous set of diseases. *Nat Rev Cancer* **14**(8): 535-546.
- Chiu CC, Haung JW, Chang FR, Huang KJ, Huang HM, Huang HW *et al.* (2013). Golden berry-derived 4beta-hydroxywithanolide E for selectively killing oral cancer cells by generating ROS, DNA damage, and apoptotic pathways. *PLoS One* **8**(5): e64739.
- Chou TC, Talalay P (1984). Quantitative analysis of dose-effect relationships: the combined effects of multiple drugs or enzyme inhibitors. *Advances in Enzyme Regulation* **22**(84): 27-55.
- Ciamporcero E, Daga M, Pizzimenti S, Roetto A, Dianzani C, Compagnone A *et al.* (2018). Crosstalk between Nrf2 and YAP contributes to maintaining the antioxidant potential and chemoresistance in bladder cancer. *Free Radic Biol Med* **115**: 447-457.
- Deep G, Oberlies NH, Kroll DJ, Agarwal R (2008). Identifying the differential effects of silymarin constituents on cell growth and cell cycle regulatory molecules in human prostate cancer cells. *Int J Cancer* **123**(1): 41-50.
- Gao S, Li S, Duan X, Gu Z, Ma Z, Yuan X *et al.* (2017). Inhibition of glycogen synthase kinase 3 beta (GSK3beta) suppresses the progression of esophageal squamous cell carcinoma by modifying STAT3 activity. *Mol Carcinog* **56**(10): 2301-2316.
- Gupte A, Mumper RJ (2009). Elevated copper and oxidative stress in cancer cells as a target for cancer treatment. *Cancer Treat Rev* **35**(1): 32-46.
- Hayes JD, Chowdhry S, Dinkova-Kostova AT, Sutherland C (2015). Dual regulation of transcription factor Nrf2 by Keap1 and by the combined actions of beta-TrCP and GSK-3. *Biochem Soc Trans* **43**(4): 611-620.
- Jiang ZQ, Li MH, Qin YM, Jiang HY, Zhang X, Wu MH (2018). Luteolin Inhibits Tumorigenesis and Induces Apoptosis of Non-Small Cell Lung Cancer Cells via Regulation of MicroRNA-34a-5p. *Int J Mol Sci* **19**(2).

Jung BJ, Yoo HS, Shin S, Park YJ, Jeon SM (2018). Dysregulation of NRF2 in Cancer: from Molecular Mechanisms to Therapeutic Opportunities. *Biomol Ther (Seoul)* **26**(1): 57-68.

Kim J, Yun M, Kim EO, Jung DB, Won G, Kim B *et al.* (2016). Decursin enhances TRAIL-induced apoptosis through oxidative stress mediated- endoplasmic reticulum stress signalling in non-small cell lung cancers. *Br J Pharmacol* **173**(6): 1033-1044.

Kim SH, Kim KY, Yu SN, Seo YK, Chun SS, Yu HS *et al.* (2016). Silibinin induces mitochondrial NOX4-mediated endoplasmic reticulum stress response and its subsequent apoptosis. *BMC Cancer* **16**: 452.

Kittiratphatthana N, Kukongviriyapan V, Prawan A, Senggunprai L (2016). Luteolin induces cholangiocarcinoma cell apoptosis through the mitochondrial-dependent pathway mediated by reactive oxygen species. *J Pharm Pharmacol* **68**(9): 1184-1192.

Kobayashi M, Yamamoto M (2005). Molecular mechanisms activating the Nrf2-Keap1 pathway of antioxidant gene regulation. *Antioxid Redox Signal* **7**(3-4): 385-394.

Latimer KM, Mott TF (2015). Lung cancer: diagnosis, treatment principles, and screening. *Am Fam Physician* **91**(4): 250-256.

Lee SB, Sellers BN, DeNicola GM (2017). The Regulation of NRF2 by Nutrient-Responsive Signaling and Its Role in Anabolic Cancer Metabolism. *Antioxid Redox Signal*.

Li C, Pan Z, Xu T, Zhang C, Wu Q, Niu Y (2014). Puerarin induces the upregulation of glutathione levels and nuclear translocation of Nrf2 through PI3K/Akt/GSK-3beta signaling events in PC12 cells exposed to lead. *Neurotoxicol Teratol* **46**: 1-9.

Liu B, Jia K, Yang Y, Hao S, Lu C, Xu F *et al.* (2017). Diosmetin Induces Cell Apoptosis by Regulating CYP1A1/CYP1A2 Due to p53 Activation in HepG2 Cells. *Protein Pept Lett* **24**(5): 406-412.

Liu B, Yu H, Baiyun R, Lu J, Li S, Bing Q, *et al.* (2018). Protective effects of dietary luteolin against mercuric chloride-induced lung injury in mice: Involvement of AKT/Nrf2 and NF-kappaB pathways. *Food Chem Toxicol* **113**: 296-302.

Liu Q, Ci X, Wen Z, & Peng L (2018). Diosmetin Alleviates Lipopolysaccharide-Induced Acute Lung Injury through Activating the Nrf2 Pathway and Inhibiting the NLRP3 Inflammasome. *Biomolecules & therapeutics* **26**: 157-166.

Martinez-Perez C, Ward C, Turnbull AK, Mullen P, Cook G, Meehan J *et al.* (2016). Antitumour activity of the novel flavonoid Oncamex in preclinical breast cancer models. *Br J Cancer* **114**(8): 905-916.

Moloney JN, Cotter TG (2017). ROS signalling in the biology of cancer. *Semin Cell Dev Biol* **80**: 50-64.

Mostafavi-Pour Z, Ramezani F, Keshavarzi F, Samadi N (2017). The role of quercetin and vitamin C in Nrf2-dependent oxidative stress production in breast cancer cells. *Oncol Lett* **13**(3): 1965-1973.

Oak C, Khalifa AO, Isali I, Bhaskaran N, Walker E, Shukla S (2018). Diosmetin suppresses human prostate cancer cell proliferation through the induction of apoptosis and cell cycle arrest. *Int J Oncol* **53**(2): 835-843.

Pan H, Zhou W, He W, Liu X, Ding Q, Ling L *et al.* (2012). Genistein inhibits MDA-MB-231 triple-negative breast cancer cell growth by inhibiting NF-kappaB activity via the Notch-1 pathway. *Int J Mol Med* **30**(2): 337-343.

Rebecca P, Riddhi P, Janmejai K, Srivastava, Sanjeev S (2016). *In-vitro* growth inhibitory effects of diosmetin on human prostate cancer cells. *cancer research* **7**(14): supplement, pp.4626.

Park KI, Park HS, Nagappan A, Hong GE, Lee DH, Kang SR *et al.* (2012). Induction of the cell cycle arrest and apoptosis by flavonoids isolated from Korean Citrus aurantium L. in non-small-cell lung cancer cells. *Food Chem* **135**(4): 2728-2735.

Rada P, Rojo AI, Chowdhry S, McMahan M, Hayes JD, Cuadrado A (2011). SCF/ β -TrCP promotes glycogen synthase kinase 3-dependent degradation of the Nrf2 transcription factor in a Keap1-independent manner. *Mol Cell Biol* **31**(6): 1121-1133.

Raza MH, Siraj S, Arshad A, Waheed U, Aldakheel F, Alduraywish S *et al.* (2017). ROS-modulated therapeutic approaches in cancer treatment. *J Cancer Res Clin Oncol* **143**(9): 1789-1809.

Rojo de la Vega M, Chapman E, Zhang DD (2018). NRF2 and the Hallmarks of Cancer. *Cancer Cell* **34**(1): 21-43.

Schumacker PT (2006). Reactive oxygen species in cancer cells: live by the sword, die by the sword. *Cancer Cell* **10**(3): 175-176.

Tang JY, Huang HW, Wang HR, Chan YC, Haung JW, Shu CW *et al.* (2018). 4beta-Hydroxywithanolide E selectively induces oxidative DNA damage for selective killing of oral cancer cells. *Environ Toxicol* **33**(3): 295-304.

Tang X, Wang H, Fan L, Wu X, Xin A, Ren H, *et al.* (2011). Luteolin inhibits Nrf2 leading to negative regulation of the Nrf2/ARE pathway and sensitization of human lung carcinoma A549 cells to therapeutic drugs. *Free radical biology & medicine* **50**: 1599-1609.

Trachootham D, Alexandre J, Huang P (2009). Targeting cancer cells by ROS-mediated mechanisms: a radical therapeutic approach. *Nat Rev Drug Discov* **8**(7): 579-591.

Wang C, Liao Y, Wang S, Wang D, Wu N, Xu Q, *et al.* (2018). Cytoprotective effects of diosmetin against hydrogen peroxide-induced L02 cell oxidative damage via activation of the Nrf2-ARE signaling pathway. *Molecular medicine reports* **17**: 7331-7338.

Wang J, Wang H, Sun K, Wang X, Pan H, Zhu J *et al.* (2018). Chrysin suppresses proliferation, migration, and invasion in glioblastoma cell lines via mediating the ERK/Nrf2 signaling pathway. *Drug Des Devel Ther* **12**: 721-733.

Wang L, Zhang S, Cheng H, Lv H, Cheng G, Ci X (2016). Nrf2-mediated liver protection by esculentoside A against acetaminophen toxicity through the AMPK/Akt/GSK3beta pathway. *Free Radic Biol Med* **101**: 401-412.

Wang Q, Wang H, Jia Y, Pan H, Ding H (2017). Luteolin induces apoptosis by ROS/ER stress and mitochondrial dysfunction in glioblastoma. *Cancer Chemother Pharmacol* **79**(5): 1031-1041.

Woo Y, Oh J, Kim JS (2017). Suppression of Nrf2 Activity by Chestnut Leaf Extract Increases Chemosensitivity of Breast Cancer Stem Cells to Paclitaxel. *Nutrients* **9** (7).

Wu Q, Yao B, Li N, Ma L, Deng Y, Yang Y *et al.* (2017). Nrf2 mediates redox adaptation in NOX4-overexpressed non-small cell lung cancer cells. *Exp Cell Res* **352**(2): 245-254.

Xu Z, Yan Y, Xiao L, Dai S, Zeng S, Qian L *et al.* (2017). Radiosensitizing effect of diosmetin on radioresistant lung cancer cells via Akt signaling pathway. *PLoS One* **12**(4): e0175977.

Ye F, Li X, Li L, Yuan J, Chen J (2016). t-BHQ Provides Protection against Lead Neurotoxicity via Nrf2/HO-1 Pathway. *Oxid Med Cell Longev* **2016**: 2075915.

Zhang C, Lan T, Hou J, Li J, Fang R, Yang Z *et al.* (2014). NOX4 promotes non-small cell lung cancer cell proliferation and metastasis through positive feedback regulation of PI3K/Akt signaling. *Oncotarget* **5**(12): 4392-4405.

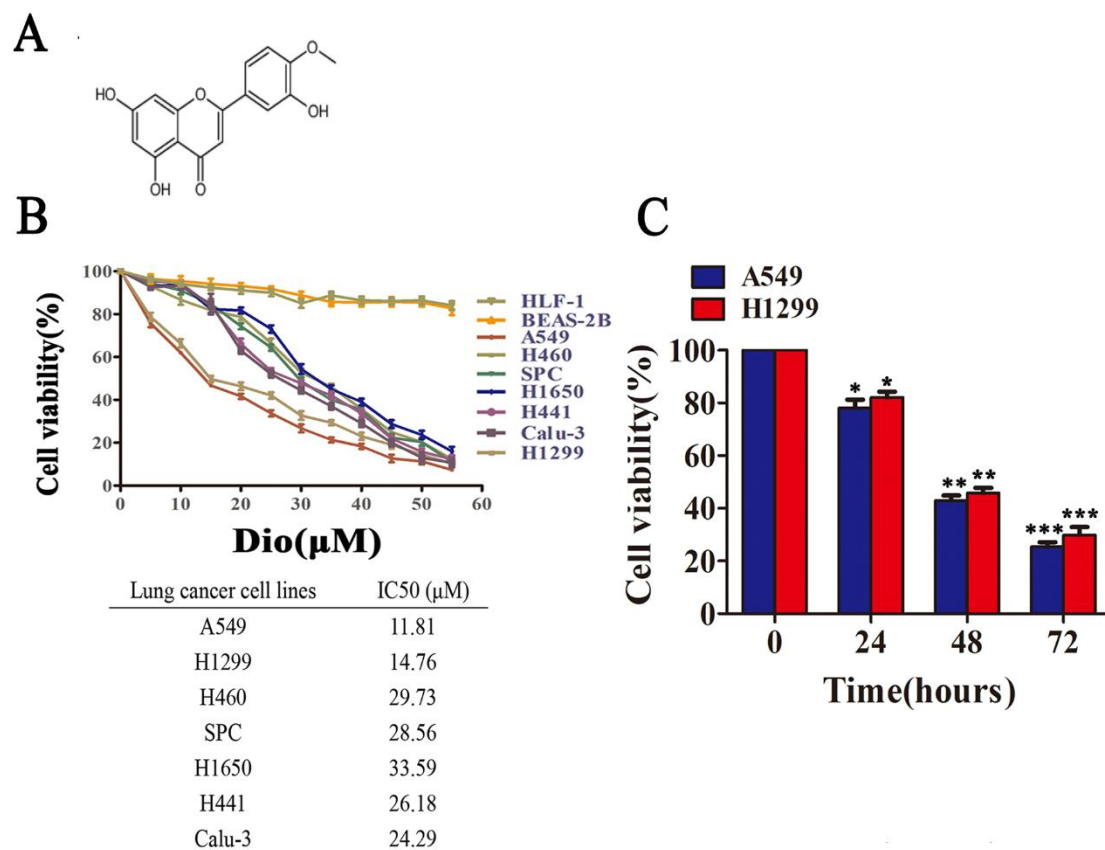


Fig.1. Diosmetin (Dio) selectively inhibits NSCLC cell viability. (A) The structure of Dio. (B) Dio treatment induces cell death in NSCLC cells, but does not induce cell death in normal cells. The effect of Dio on the viability of the NSCLC cells A549, H1299, H441, H460, SPC, Calu-3, H1650 and the normal cells HLF-1 and BEAS-2B by MTT assay at the indicated concentration, $n=5$. The IC₅₀ (mean \pm S.D.) of Dio against tumor cell lines. (C) Time-dependent of Dio on the viability of the A549 and H1299 cells as assessed by MTT. * $p < 0.05$, ** $p < 0.01$ and *** $p < 0.001$, significantly different from control group, $n=5$.

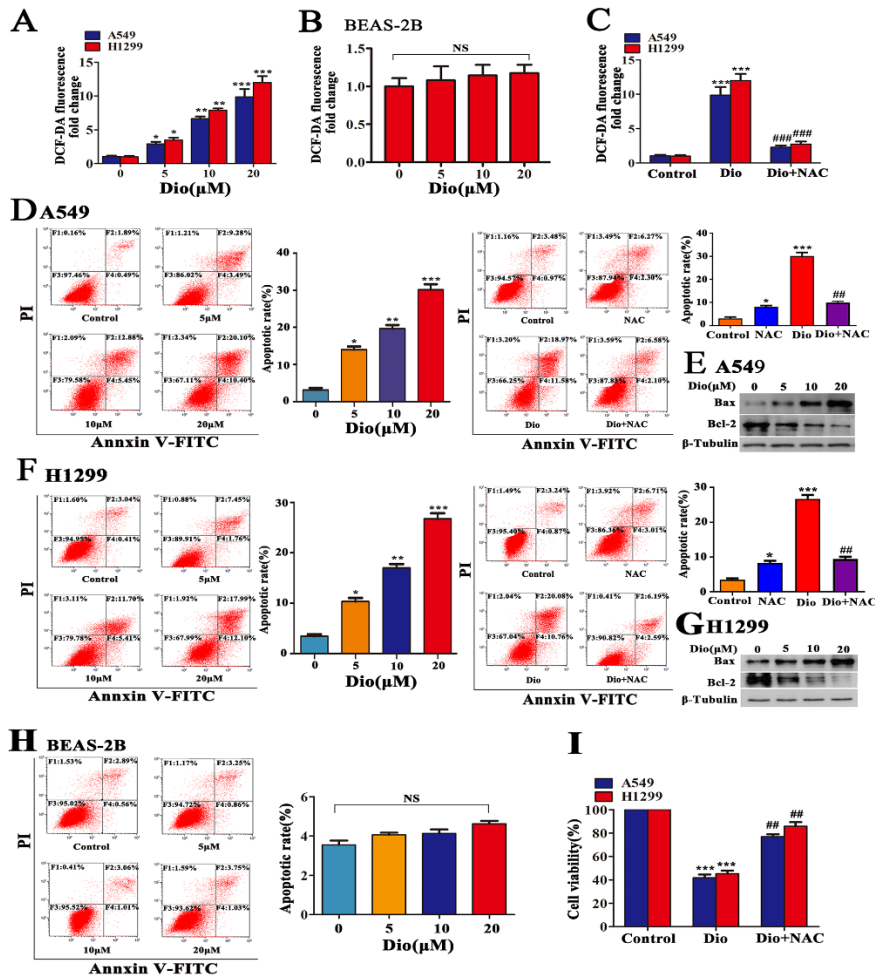


Fig.2. Dio induces cell apoptosis via cellular ROS accumulation. The effect of Dio at the indicated concentrations on ROS production in A549 and H1299 cells (A) and BEAS-2B cells (B). ROS accumulation abrogated by administration of a ROS scavenger NAC (25 mM) (C) examined by DCF-DA fluorescence assay. Significantly different from control group, * $p < 0.05$, ** $p < 0.01$, *** $p < 0.001$ and #### $p < 0.001$, $n = 5$; #significantly different from the group of Dio plus NAC, $P < 0.001$, $n = 5$. The effect of Dio (5 to 20 μ M) treatment for 12 hours on A549 (D) and H1299 (F) cells apoptosis, the administration of NAC (25 mM) efficiently reversed the effect of Dio (20 μ M) on by cell apoptosis determined by flow cytometry. Significantly different from control group, * $p < 0.05$, ** $p < 0.01$ and *** $p < 0.001$, $n = 5$; ##significantly different from the group of Dio+NAC plus Dio, $P < 0.01$, $n = 5$. (E and G) Dio (5 to 20 μ M) promoted Bax and suppressed Bcl-2 expression in A549 and H1299 cells analyzed by western blotting after 12 hours incubation. (H) The effect of Dio (5 to 20 μ M) treatment for 12 hours on BEAS-2B cell apoptosis determined by flow cytometry. NS, not significantly, $n = 5$. Administration of NAC (25 mM) efficiently reversed the effect of Dio (20 μ M) on A549 and H1299 cells viability determined by MTT (I). Significantly different from control group, *** $p < 0.001$ and ** $p < 0.01$, $n = 5$; #significantly different from the group of Dio plus NAC.

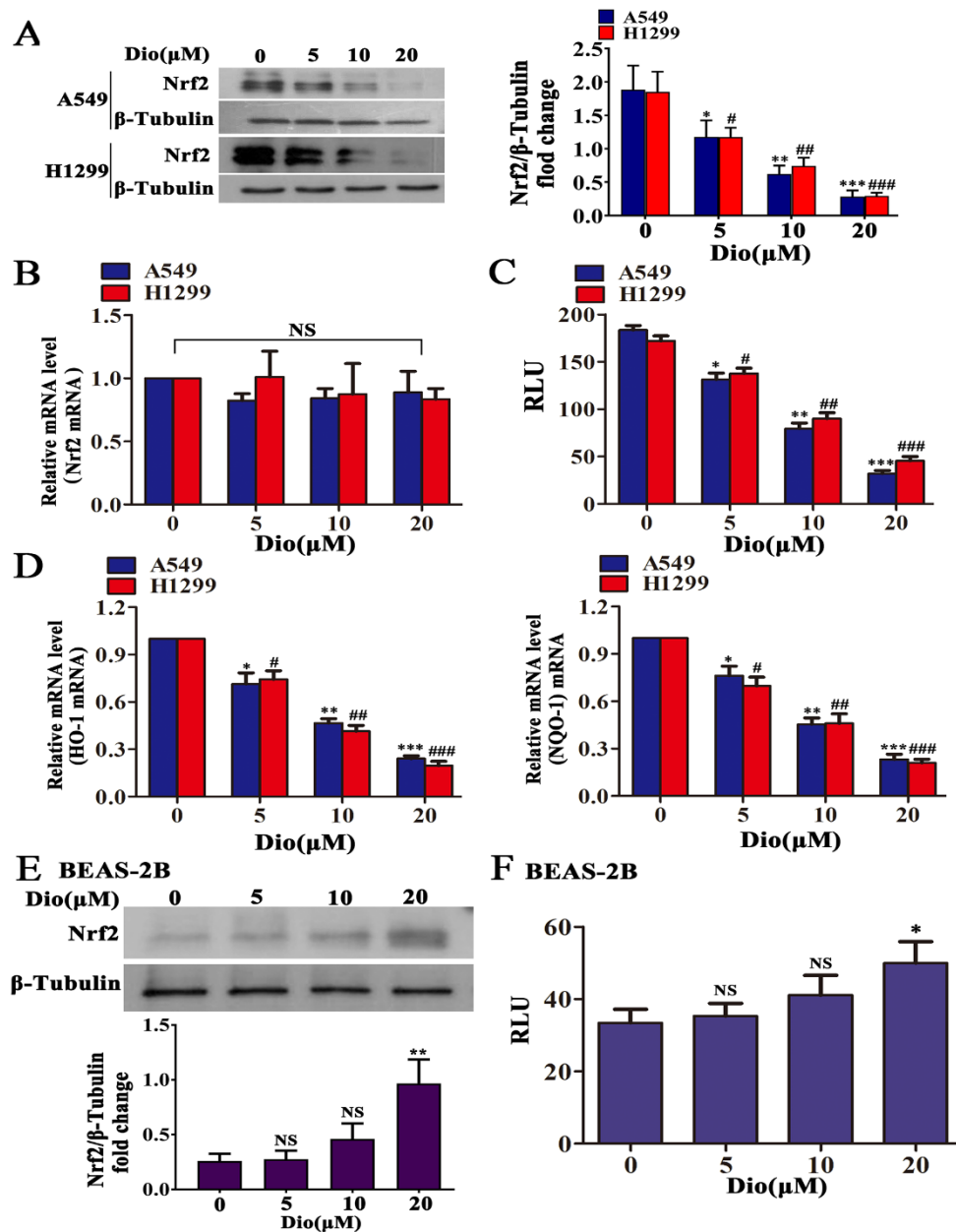


Fig.3. Interference of Nrf2 expression mediates Dio-induced NSCLC apoptosis. (A) Dio (5 to 20 μM) suppressed Nrf2 expression in A549 and H1299 cells analyzed by western blotting after 12 hours incubation. (B) The effect of Dio on Nrf2 mRNA expression in A549 and H1299 cells assayed by Q-PCR. Significantly different from control group, NS, not significantly, $n=5$. (C) Dio decreased RLU activity ($\times 10^4$) in A549 and H1299 cells at the indicated concentration after 12 hours treatment. Significantly different from control group, $*p < 0.05$, $**p < 0.01$ and $***p < 0.001$, $n=5$. (D) The effect of Dio on the mRNA expression of Nrf2-targeted genes (HO-1 and NQO-1) in A549 and H1299 cells determined by Q-PCR. Significantly different from control group, $*p < 0.05$, $**p < 0.01$ and $***p < 0.001$, $n=5$. The effect of Dio (5 to 20 μM) treatment for 12 hours on BEAS-2B cell Nrf2 expression analyzed by western blotting. (E) and RLU activity ($\times 10^4$) (F). Significantly different from control group, $*p < 0.05$, NS, not significantly, $n=5$.

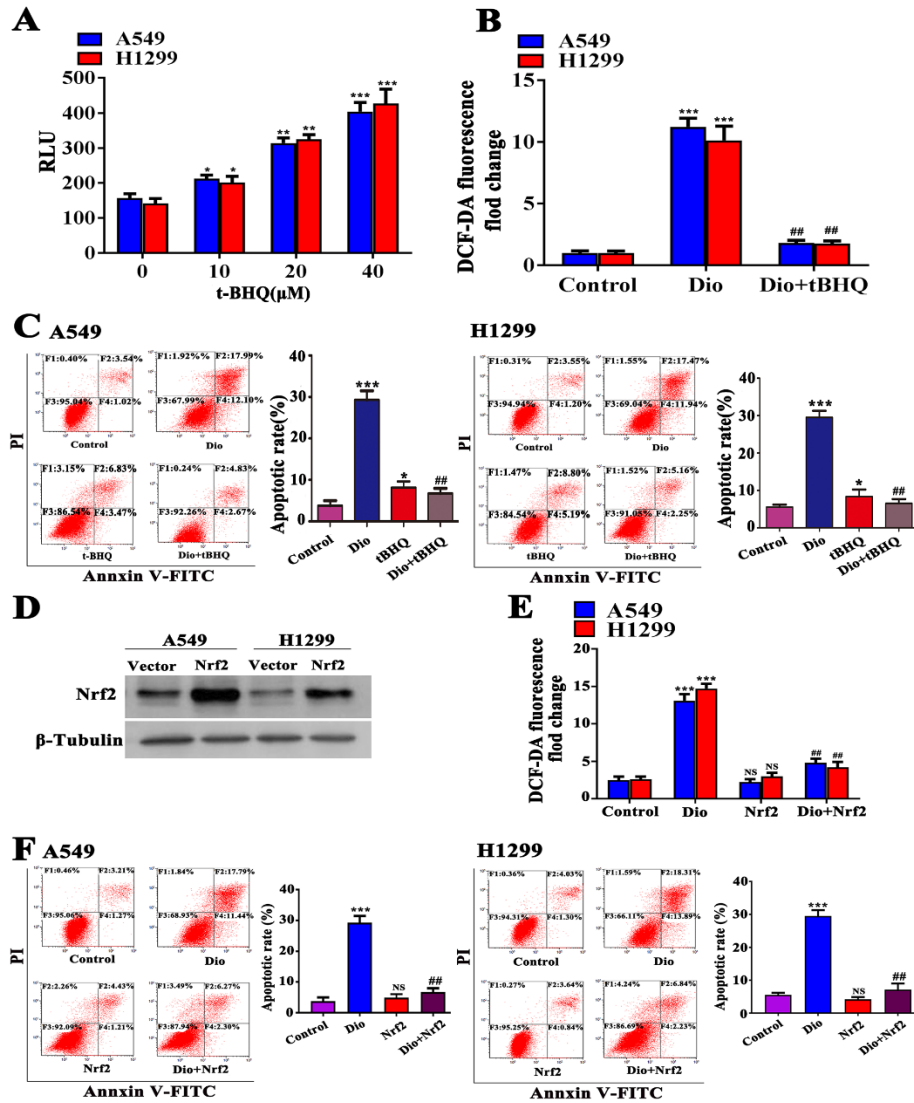


Fig.4. tBHQ reverses Dio-induced A549 and H1299 cells apoptosis and ROS production. (A) tBHQ (10 to 40 μ M) increased Nrf2 activity ($\times 10^4$) in a dose-dependent manner in A549 and H1299 cells determined by ARE-luciferase report assay. Significantly different from control group, $*p < 0.05$, $**p < 0.01$ and $***p < 0.001$, $n = 5$. tBHQ (20 μ M) reversed Dio-induced ROS accumulation (B). Significantly different from control group, $**p < 0.01$ and $***p < 0.001$; #significantly different from the group of Dio plus tBHQ (20 μ M), $p < 0.01$, $n = 5$. (C) tBHQ (20 μ M) blocked Dio (20 μ M)-induced apoptosis in A549 and H1299 cells. Significantly different from control group, $**p < 0.01$ and $***p < 0.001$; #significantly different from the group of Dio plus tBHQ (20 μ M), $p < 0.01$, $n = 5$. (D) Nrf2 overexpression in A549 and H1299 cells analyzed by western blotting after 12 hours incubation. Overexpression reversed Nrf2-induced ROS accumulation (E), Significantly different from control group, $**p < 0.01$ and $***p < 0.001$; #significantly different from the group of Dio+Nrf2 plus Dio, $p < 0.01$, $n = 5$. (F) Overexpression Nrf2 blocked Dio (20 μ M)-induced apoptosis in A549 and H1299 cells. Significantly different from control group, $**p < 0.01$ and $***p < 0.001$; #significantly different from the group of Dio+Nrf2 plus Dio, $p < 0.01$, $n = 5$

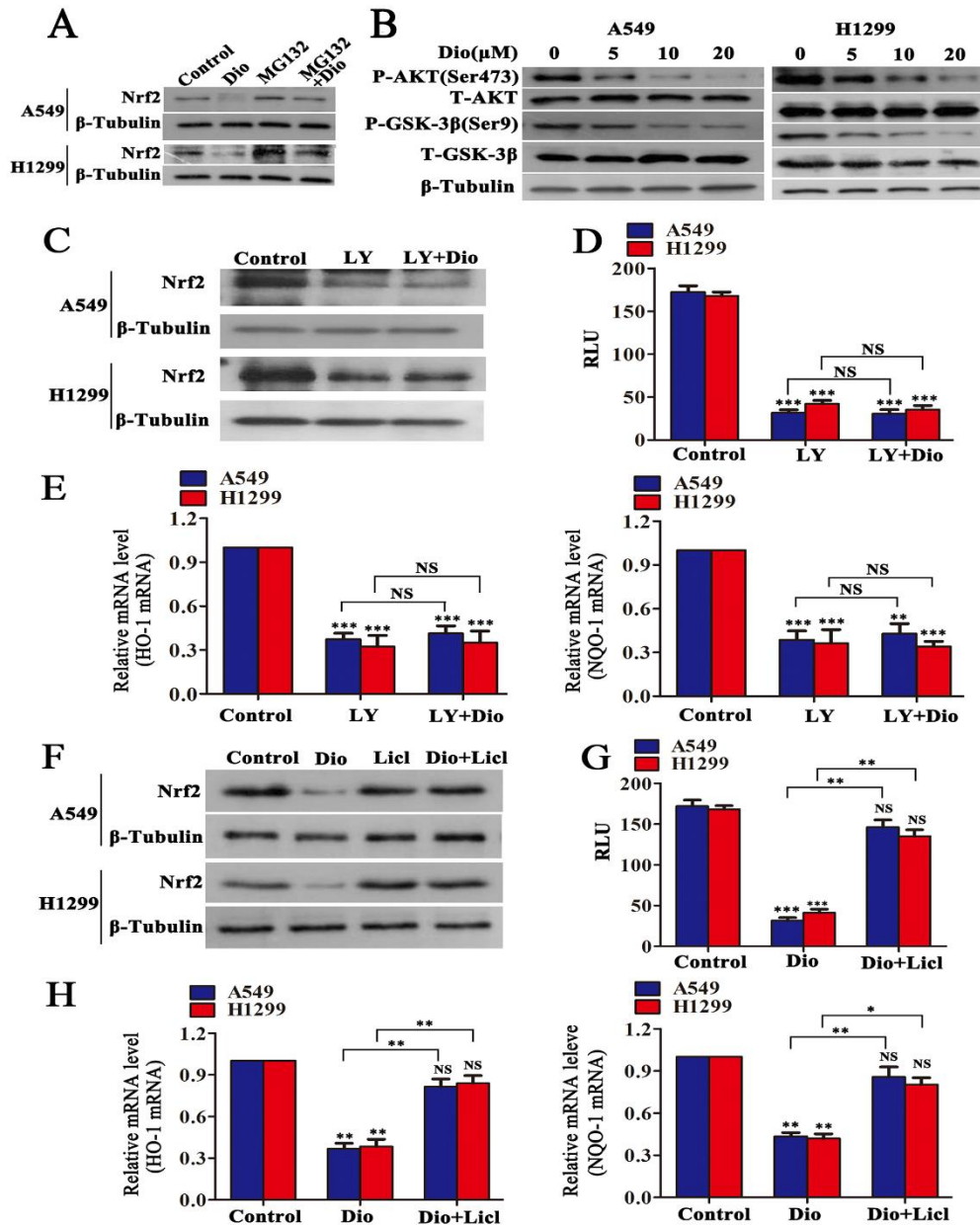


Fig.5. Dio attenuates Nrf2 expression in NSCLC cells via inhibition of PI3K/Akt/GSK-3 β pathway. (A) The effects of MG132 alone on Nrf2 expression or on Dio-reduced Nrf2 expression determined by western blotting. (B) Dio inhibited phosphorylated Akt and phosphorylated GSK-3 β levels in A549 and H1299 cells analyzed by western blotting after 12 hours treatment. (C-E) After administration of LY294002 and LY294002 plus Dio, the expression of Nrf2 and RLU ($\times 10^4$) and the mRNA expression of Nrf2-targeted genes (HO-1 and NQO-1) in A549 and H1299 cells was analyzed by western blotting, ARE-luciferase report and Q-PCR assayed. Significantly different from control group, *** $p < 0.001$; NS, not significantly, $n = 5$. (F-H) After administration of Dio and Dio plus Licl, licl efficiently reversed the effect of the expression of Nrf2 and RLU ($\times 10^4$) and the mRNA expression of Nrf2-targeted genes (HO-1 and NQO-1) in A549 and H1299 cells was analyzed by western blotting, ARE-luciferase report and Q-PCR assayed. Significantly different from control group, * $p < 0.05$, ** $p < 0.01$ and *** $p < 0.001$; NS, not significantly, $n = 5$.

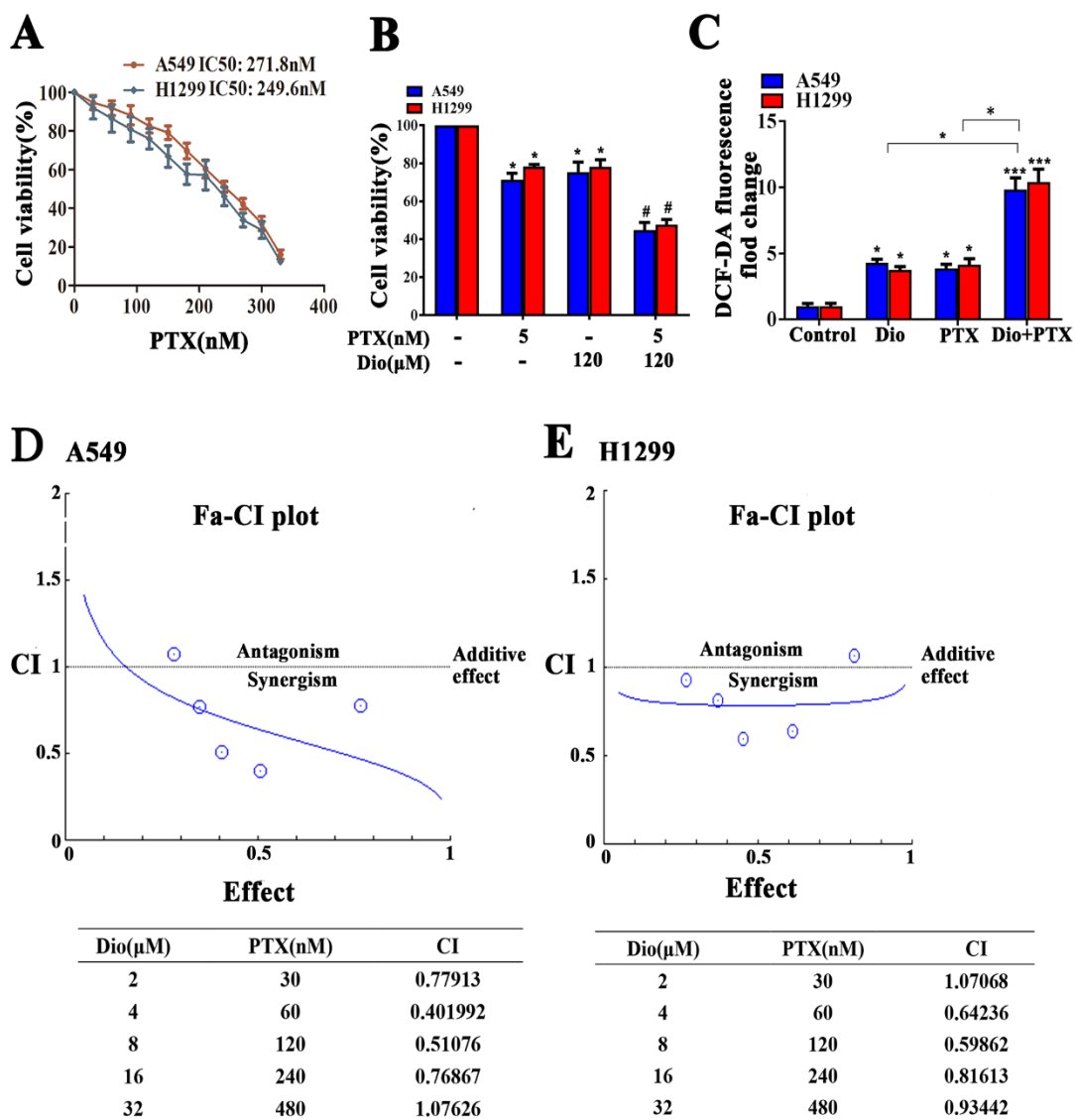


Fig.6. Dio enhances paclitaxel cytotoxicity in NSCLC cells. (A) Cell viability assessed by MTT after treatment with PTX at the indicated concentrations. n=5. (B) Combined effect of Dio and PTX in A549 and H1299 cells determined by MTT assay. A549 and H1299 cells were exposed to different concentration of Dio and PTX for 48h. (C) Combined of the ROS production Dio and PTX in A549 and H1299 cells examined by DCF-DA fluorescence assay. Significantly different from control group, * $p < 0.05$, ** $p < 0.01$ and *** $p < 0.001$, n=5. Combination index analysis of the induction of differentiation in A549 (D) and H1299 (E) cells treated with the combination of Dio and PTX. A combination index of 1.0 reflects additive effects, whereas values greater than and less than 1.0 indicate antagonism and synergy, respectively.

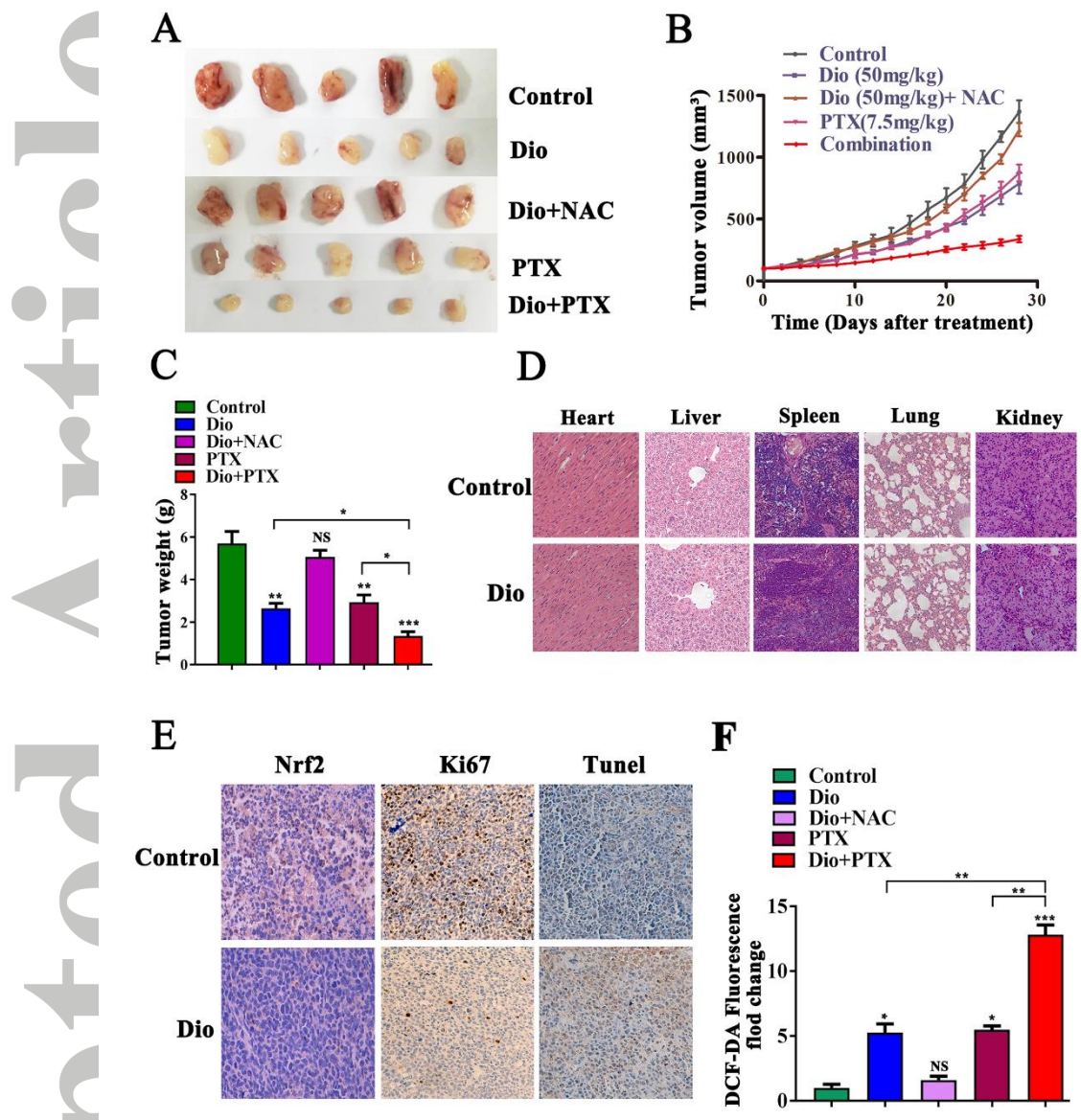


Fig.7. Dio impairs A549 cells and enhances paclitaxel efficacy *in vivo*. Dio (50 mg/kg, thrice weekly, by intraperitoneal injection); Dio plus the NAC (7 mg/ml given in the drinking water for the length of the experiment); PTX (10 mg/kg, thrice weekly, by intraperitoneal injection) and Dio plus the PTX treatment inhibit tumor volume (A-B) and tumor weight (C). Histopathologic analyses of major organs from control and Dio treatment group (D). (E) The tumor tissues were stained with antibody to Nrf2 and ki67, respectively. Apoptotic nuclei with fragmented DNA were detected by TUNEL staining. Magnification, 20 \times . The positive staining of Nrf2 expression per field from paraffin-embedded sections of control cells or those treated with Dio was determined by immunohistochemistry and morphometric quantification. Significantly different from control group, $**p < 0.01$. (F) Tumor tissues ROS level. Significantly different from control group, $*p < 0.05$, $**p < 0.01$ and $***p < 0.001$, NS, not significantly, $n=5$.

Graphical Abstract

Diosmetin selectively induces ROS accumulation and cell death, as well as enhances the antitumor efficacy of paclitaxel in NSCLC cells by interfering with Nrf2 antioxidant defense mechanisms through disruption of PI3K/Akt/GSK-3 β pathway.

